Inorganic Chemistry

Article

pubs.acs.org/IC

Octahedral Co-Carbide Carbonyl Clusters Decorated by $[AuPPh_3]^+$ Fragments: Synthesis, Structural Isomerism, and Aurophilic Interactions of $Co_6C(CO)_{12}(AuPPh_3)_4$

Iacopo Ciabatti,[†] Cristina Femoni,[†] Mohammad Hayatifar,[†] Maria Carmela Iapalucci,[†] Andrea Ienco,[‡] Giuliano Longoni,[†] Gabriele Manca,[‡] and Stefano Zacchini*[,†]

[†]Dipartimento di Chimica Industriale "Toso Montanari", Università di Bologna, Viale Risorgimento 4 − 40136 Bologna, Italy

[‡]Consiglio Nazionale delle Ricerche—Istituto di Chimica dei Composti Organo Metallici, Via Madonna del Piano 10 − 50019, Sesto Fiorentino, Firenze, Italy

Supporting Information

ABSTRACT: The $Co_6C(CO)_{12}(AuPPh_3)_4$ carbide carbonyl cluster was obtained from the reaction of $[Co_6C(CO)_{15}]^{2-}$ with $Au(PPh_3)Cl$. This new species was investigated by variable-temperature ^{31}P NMR spectroscopy, X-ray crystallography, and density functional theory methods. Three different solvates were characterized in the solid state, namely, $Co_6C(CO)_{12}(AuPPh_3)_4$ (**I**), $Co_6C(CO)_{12}(AuPPh_3)_4$·THF (**II**), and $Co_6C(CO)_{12}(AuPPh_3)_4$·4THF (**III**), where THF = tetrahydrofuran. These are not merely different solvates of the same neutral cluster, but they contain three different isomers of $Co_6C(CO)_{12}(AuPPh_3)_4$. The three isomers **I**−**III** possess the same octahedral $[Co_6C(CO)_{12}]^{4-}$ carbido−carbonyl core differently decorated by four $[AuPPh_3]^+$ fragments and showing a different Au(I)···Au(I) connectivity. Theoretical investigations suggest that the formation in the solid state of the three isomers during crystallization is governed by packing and van der Waals forces, as well as aurophilic and weak $\pi-\pi$ and π−H interactions. In addition, the closely related cluster $Co_6C(CO)_{12}(PPh_3)(AuPPh_3)_2$ was obtained from the reaction of $[Co_8C(CO)_{18}]^{2-}$ with $Au(PPh_3)Cl$, and two of its solvates were crystallographically characterized, namely, $Co_6C(CO)_{12}(PPh_3)(AuPPh_3)_2$·toluene (**IV**) and $Co_6C(CO)_{12}(PPh_3)(AuPPh_3)_2$·0.5toluene (**V**). A significant, even if minor, effect of the cocrystallized solvent molecules on the structure of the cluster was observed also in this case.

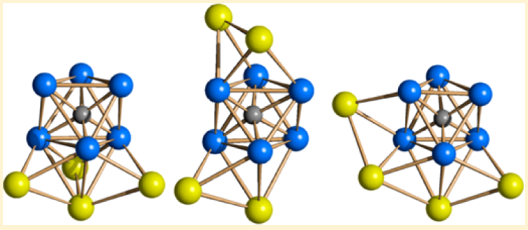

1. INTRODUCTION

Several M_6C carbide−carbonyl clusters are known. Usually, species possessing 86 cluster valence electrons (CVE) are octahedral, whereas clusters with 90 CVE adopt a trigonal prismatic structure, even if exceptions have been described.[1−4] This is well-exemplified in the chemistry of cobalt−carbide clusters, for which the electron precise trigonal prismatic $[Co_6C(CO)_{15}]^{2-}$ (90 CVE) and octahedral $[Co_6C(CO)_{13}]^{2-}$ (86 CVE) species have been known for decades.[5,6] In addition, an octahedral structure is adopted also by the paramagnetic electron-rich $[Co_6C(CO)_{14}]^-$ (87 CVE) and electron-poor $[Co_6C(CO)_{12}]^{3-}$ (85 CVE) clusters.[7,8]

The metal cage of anionic metal carbonyl clusters may behave as a soft Lewis base, whereas hard acids prefer to react at the O atoms of the CO ligands.[9,10] Au(I) fragments have been widely employed as soft Lewis acids toward anionic metal carbonyl clusters.[11−13] In most cases, the Au(I) reagent has been added to preformed anionic carbonyls to selectively expand of a few units the nuclearity of the cluster. In other cases, based on the isolobal analogy between $[AuL]^+$ and H^+, the former fragments have been used to have information on the protonation sites of anionic metal carbonyl clusters.[14,15] Alternatively, coordination to cationic metal centers may lead to the stabilization and, eventually, isolation of unprecedented clusters.[16−18]

We have previously shown that the octahedral M_6C framework is a good platform to test aurophilicity.[19] This is rather stable and rigid supporting the possibility, upon coordination of two or more $[AuPPh_3]^+$ fragments, of having isomers which differ in the weaker $d^{10}-d^{10}$ Au(I)···Au(I) interactions. In view of the widespread interest in such aurophilic interactions,[20−25] we herein report the synthesis and structural characterization of three different isomers of the unprecedented $Co_6C(CO)_{12}(AuPPh_3)_4$ cluster. These contain the same $[Co_6C(CO)_{12}]^{4-}$ octahedral core, to which four $[AuPPh_3]^+$ fragments are differently coordinated. IR and variable-temperature ^{31}P NMR spectroscopies indicate that dissociation of two $[AuPPh_3]^+$ fragments occurs in solution, and the different isomers are formed due to condensation occurring during crystallization. The free $[Co_6C(CO)_{12}]^{4-}$ cluster is not known, whereas the closely related paramagnetic $[Co_6C(CO)_{12}]^{3-}$ species has been recently characterized.[8]

Prior to this work, the only octahedral Co−carbide carbonyl clusters containing $[AuPPh_3]^+$ fragments structurally characterized were $Co_6C(CO)_{13}(AuPPh_3)_2$ and $[Co_6C(CO)_{13}(AuPPh_3)]^-$, whereas $[Co_6C(CO)_{12}(AuPPh_3)_2]^{2-}$ was

Received: June 9, 2014
Published: August 28, 2014

   dx.doi.org/10.1021/ic501346a | *Inorg. Chem.* 2014, 53, 9761−9770

only spectroscopically identified.[26] As an additional result of our present investigation, we will herein describe also the $Co_6C(CO)_{12}(PPh_3)(AuPPh_3)_2$ derivative, which is formally obtained from $Co_6C(CO)_{13}(AuPPh_3)_2$ after replacing one CO ligand with PPh_3.

2. RESULTS AND DISCUSSION

2.1. Synthesis of $Co_6C(CO)_{12}(AuPPh_3)_4$ and $Co_6C(CO)_{12}(PPh_3)(AuPPh_3)_2$. The new neutral cluster $Co_6C(CO)_{12}(AuPPh_3)_4$ was obtained by reacting $[Co_6C(CO)_{15}]^{2-}$ with 2−3 equiv of $Au(PPh_3)Cl$, in accord with eqs 1 and 2, respectively:

$$2[Co_6C(CO)_{15}]^{2-} + 4Au(PPh_3)Cl \rightarrow Co_6C(CO)_{12}(AuPPh_3)_4 + C + 4[Co(CO)_4]^- + 2Co^{2+} + 2CO + 4Cl^- \quad (1)$$

$$6[Co_6C(CO)_{15}]^{2-} + 18Au(PPh_3)Cl \rightarrow 3Co_6C(CO)_{12}(AuPPh_3)_4 + 3C + 10[Co(CO)_4]^- + 8Co^{2+} + 14CO + 18Cl^- + 6Au + 6PPh_3 \quad (2)$$

The side-products $[Co(CO)_4]^-$ and Co^{2+} have been identified by IR spectroscopy and the typical pink color of the water extract during workup, respectively. Formation of a gold mirror on the reaction flask was also observed. The neutral cluster was purified by removing the solvent *in vacuo*, washing the residue with water and toluene, and finally extracted in tetrahydrofuran (THF). Crystallization by slow diffusion of *n*-hexane on the THF solutions affords three types of crystals, namely, $Co_6C(CO)_{12}(AuPPh_3)_4$ (**I**), $Co_6C(CO)_{12}(AuPPh_3)_4$·THF (**II**), and $Co_6C(CO)_{12}(AuPPh_3)_4$·4THF (**III**), as single species and/or mixtures, depending on the experimental conditions (concentration, rate of diffusion, amount of *n*-hexane). The use of toluene/*n*-hexane instead of THF/*n*-hexane for crystallization results in crystals of **I** as well as $Co_6C(CO)_{12}(AuPPh_3)_4$·4toluene closely related to **III**. Conversely, crystallization from CH_2Cl_2/*n*-hexane affords crystal of **I**. It is noteworthy that they are not merely different solvates of the same neutral cluster, but they contain three different isomers of $Co_6C(CO)_{12}(AuPPh_3)_4$ (see Section 2.2). As discussed in the next section, all three isomers contain the same octahedral $[Co_6C(CO)_{12}]^{4-}$ carbido−carbonyl core differently decorated by four $[AuPPh_3]^+$ fragments. As a consequence, the three crystals display different IR spectra in nujol mull. Thus, $Co_6C(CO)_{12}(AuPPh_3)_4$ (**I**) displays ν(CO) at 2034(s), 2004(vs), 1966(s), 1921(vs), 1879(sh), and 1799(vs) cm^{-1}, whereas $Co_6C(CO)_{12}(AuPPh_3)_4$·THF (**II**) shows ν(CO) at 2009(vs), 1980(s), 1941(m), 1834(m), and 1812(m) cm^{-1} and $Co_6C(CO)_{12}(AuPPh_3)_4$·4THF (**III**) shows ν(CO) at 2022(m), 2008(m), 1965(s), 1939(w), 1875(w), 1857(w), 1834(w), 1821(m), and 1796(w) cm^{-1}.

Crystals of **I**−**III** are poorly soluble in organic solvents, and in all cases, after dissolution they dissociate two $[AuPPh_3]^+$ fragments resulting in the previously reported $[Co_6C(CO)_{12}(AuPPh_3)_2]^{2-}$ anion (eq 3), which has been identified by means of IR spectroscopy (ν(CO) at 1942(vs), 1810(m) cm^{-1} in THF):[26]

$$Co_6C(CO)_{12}(AuPPh_3)_4 \rightleftarrows [Co_6C(CO)_{12}(AuPPh_3)_2]^{2-} + 2[AuPPh_3]^+ \quad (3)$$

Equilibrium 3 seems to explain why it is not possible to uniquely form a single isomer in a controlled manner. Thus, in solution the cluster is mostly ionized, and $[Co_6C(CO)_{12}(AuPPh_3)_2]^{2-}$ condenses with two $[AuPPh_3]^+$ during crystallization leading to the different isomeric forms of $Co_6C(CO)_{12}(AuPPh_3)_4$, depending on the experimental conditions, for example, concentration, rate of diffusion, and solvents employed.

The presence in solution of dynamic equilibria has been demonstrated by variable temperature $^{31}P\{^1H\}$ NMR experiments (Figure 1). Two resonances at δ_P 49.1 (br) and 47.8 (s)

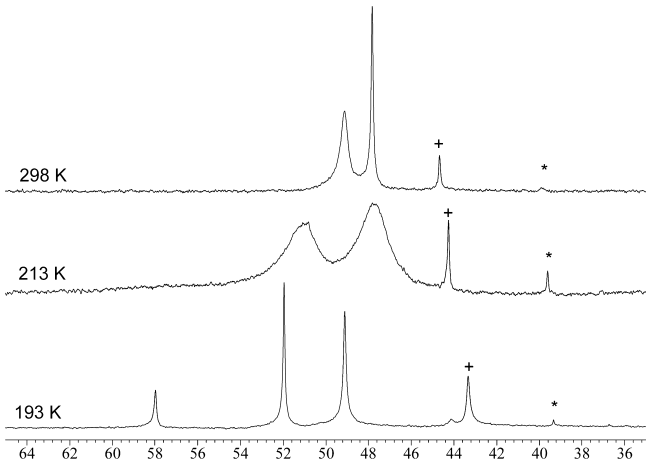

Figure 1. Variable-temperature $^{31}P\{^1H\}$ NMR spectra of $Co_6C(CO)_{12}(AuPPh_3)_4$ in CD_2Cl_2. (+) and (*) are impurities.

ppm are present at 298 K, which broaden by lowering the temperature. The exchange is frozen at 193 K, as demonstrated by the presence of three sharp singlets at (relative intensities are given in parentheses) δ_P 49.1 (351), 51.9 (274), and 58.0 (100) ppm. The resonance at 51.9 ppm may be assigned to $[Co_6C(CO)_{12}(AuPPh_3)_2]^{2-}$ by comparison to literature data.[26] The resonance at 58.0 ppm may be tentatively assigned to a more dissociated $[Co_6C(CO)_{12}(AuPPh_3)]^{3-}$ species (eq 4):

$$[Co_6C(CO)_{12}(AuPPh_3)_2]^{2-} \rightleftarrows [Co_6C(CO)_{12}(AuPPh_3)]^{3-} + [AuPPh_3]^+ \quad (4)$$

This is in agreement with the fact that a shift toward higher frequencies has been previously observed for $Co_6C(CO)_{13}(AuPPh_3)_2$ (δ_P 50.2 ppm) upon dissociation to $[Co_6C(CO)_{13}(AuPPh_3)]^-$ (δ_P 54.0 ppm).[26] The major resonance at 49.1 ppm may be assigned to $[AuPPh_3]^+$, which is generated by the occurrence in solution of both equilibria 3 (completely shifted to the right in solution) and 4. By comparison, $Au(PPh_3)Cl$ shows under the same experimental conditions a singlet at δ_P 33.1 ppm. Addition of small amounts of $Au(PPh_3)Cl$ ($\leq$1 equiv) to the above solution results in the appearance of a singlet at δ_P 33.1 ppm without shifting the equilibria. Further addition of the Au(I) reagent leads to complete decomposition of the cluster.

In the search of other Co_6C carbonyl clusters containing $[AuPPh_3]^+$ fragments, different experimental conditions such as reagents, solvent, temperature, and stoichiometric ratios were attempted, usually leading to very complex mixtures of products not yet identified. During these attempts, while studying the reaction in CH_2Cl_2 of $[Co_6C(CO)_{15}]^{2-}$ with 1 equiv of $Au(PPh_3)Cl$ in the presence of free PPh_3 (2 equiv) and $AgNO_3$ (1 equiv) a few crystals of $Co_6C(CO)_{12}(PPh_3)(AuPPh_3)_2$·toluene (**IV**) were obtained. It must be remarked that the homoleptic analogous $Co_6C(CO)_{13}(AuPPh_3)_2$ has been previously reported in the literature.[26] The crystals of Co_6C-

dx.doi.org/10.1021/ic501346a | Inorg. Chem. 2014, 53, 9761−9770

$(CO)_{12}(PPh_3)(AuPPh_3)_2$·toluene (**IV**) displays ν(CO) in nujol mull at 2041(m), 1999(s), 1984(sh), 1953(s), 1856(m), and 1830(m) cm^{-1}. Nonetheless, the above synthesis gives $Co_6C(CO)_{12}(PPh_3)(AuPPh_3)_2$·toluene (**IV**) only as the minor product, whereas the main products formed have not been yet identified. Thus, seeking a better synthesis of this compound, we have studied the reaction of $[Co_8C(CO)_{18}]^{2-}$ with $Au(PPh_3)Cl$. The best results have been obtained using three equivalents of the Au(I) reagent per mole of cluster anion, in agreement with eq 5:

$$[Co_8C(CO)_{18}]^{2-} + 3Au(PPh_3)Cl \rightarrow Co_6C(CO)_{12}(PPh_3)(AuPPh_3)_2 + [Co(CO)_4]^- + Co^{2+} + 2CO + 3Cl^- + Au \quad (5)$$

After workup of the reaction mixture (see Experimental Section), the neutral cluster was extracted in toluene and crystals of $Co_6C(CO)_{12}(PPh_3)(AuPPh_3)_2$·0.5toluene (**V**) were obtained by slow diffusion of *n*-hexane. As described in Section 2.3, **IV** and **V** contain the same $Co_6C(CO)_{12}(PPh_3)(AuPPh_3)_2$ cluster with only some minor (but yet significant) differences, mainly due to packing effects.

Crystals of **V** show ν(CO) in nujol mull at 2056(w), 2035(w), 1997(vs), 1980(sh), 1953(s), 1859(w), 1829(m), and 1801(sh) cm^{-1}. The IR spectra in nujol mull of **IV** and **V** are slightly different, in view of the minor structural differences found in their solid-state structures (Section 2.3).

Crystals of **V** are soluble in toluene, where they show ν(CO) at 2059(w), 2008(s), 1958(w), and 1848(w) cm^{-1}. These are sensibly lower than the ν(CO) bands reported for $Co_6C(CO)_{13}(AuPPh_3)_2$ (2059(m), 2019(vs), and 1858(m) cm^{-1}), in view of the replacement of one CO ligand with the stronger PPh_3 base. Partial dissociation to $[Co_6C(CO)_{12}(PPh_3)(AuPPh_3)]^-$ (ν(CO) at 2057(w), 1978(s), 1953(w), and 1813(w) cm^{-1} in THF) occurs in more polar solvents, such as THF. For comparison, the previously reported $[Co_6C(CO)_{13}(AuPPh_3)]^-$ displays ν(CO) at 2041(m), 1989(vs), and 1824(m) cm^{-1}. Complete dissociation, then, occurs by further increasing the polarity of the solvent, for example, by using CH_3CN or dimethylformamide (DMF), resulting in the formation of $[Co_6C(CO)_{12}(PPh_3)]^{2-}$, ν(CO) at 1970(w), 1941(vs), and 1806(s) cm^{-1} in DMF. Compare to $[Co_6C(CO)_{13}]^{2-}$ ν(CO) at 1968(vs) and 1816(m) cm^{-1} in acetone.

$$Co_6C(CO)_{12}(PPh_3)(AuPPh_3)_2 \rightleftarrows [Co_6C(CO)_{12}(PPh_3)(AuPPh_3)]^- + [Au(PPh_3)]^+ \quad (6)$$

$$[Co_6C(CO)_{12}(PPh_3)(AuPPh_3)]^- \rightleftarrows [Co_6C(CO)_{12}(PPh_3)]^{2-} + [Au(PPh_3)]^+ \quad (7)$$

Variable-temperature $^{31}P\{^1H\}$ NMR experiments on $Co_6C(CO)_{12}(PPh_3)(AuPPh_3)_2$ dissolved in CD_2Cl_2, where there is not significant dissociation, indicate that the cluster is fluxional in solution (Figure 2). Thus, a sharp singlet at 41.8 ppm and a very broad resonance centered at 43 ppm are present at 298 K, which become two broad resonances at 43.1 and 41.0 ppm at 193 K. These may be assigned to the PPh_3 ligand bonded to Au and Co, respectively.

2.2. Crystal Structures of the Isomers of $Co_6C(CO)_{12}(AuPPh_3)_4$ as Found in $Co_6C(CO)_{12}(AuPPh_3)_4$ (I), $Co_6C(CO)_{12}(AuPPh_3)_4$·THF (II), $Co_6C(CO)_{12}(AuPPh_3)_4$·4THF (III).

The structure of the neutral $Co_6C(CO)_{12}(AuPPh_3)_4$ cluster

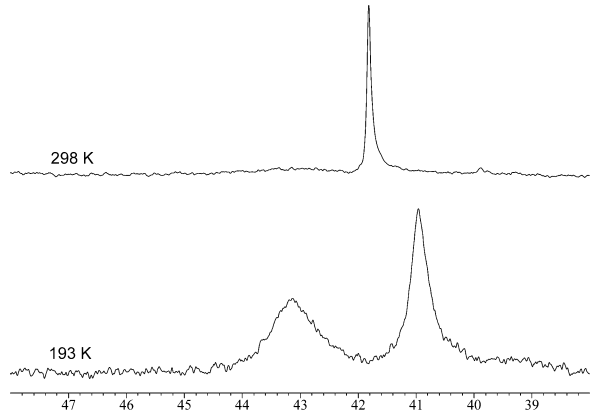

Figure 2. Variable temperature $^{31}P\{^1H\}$ NMR spectra of $Co_6C(CO)_{12}(PPh_3)(AuPPh_3)_2$ in CD_2Cl_2.

was determined as its $Co_6C(CO)_{12}(AuPPh_3)_4$ (**I**), $Co_6C(CO)_{12}(AuPPh_3)_4$·THF (**II**), and $Co_6C(CO)_{12}(AuPPh_3)_4$·4THF (**III**) solvates (Figures 3−5 and Table 1). It must be

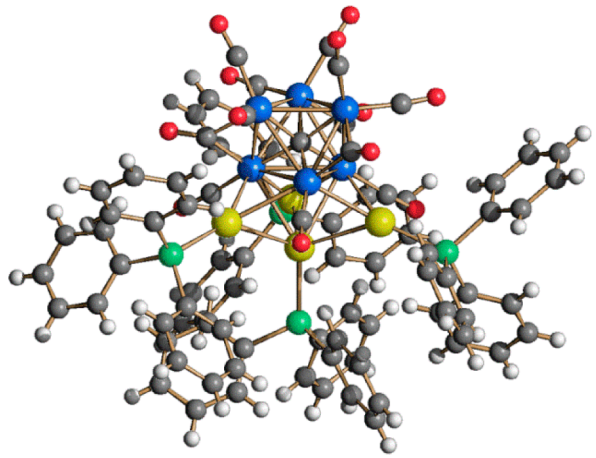

Figure 3. Molecular structure of $Co_6C(CO)_{12}(AuPPh_3)_4$ (isomer **I**) as found in $Co_6C(CO)_{12}(AuPPh_3)_4$ (blue, Co; yellow, Au; green, P; red, O; gray, C; white, H).

remarked that they differ not only because of the solvent molecules, but more importantly, they contain three different isomers of $Co_6C(CO)_{12}(AuPPh_3)_4$. It seems likely that the formation in the solid state of the three isomers during crystallization is governed by packing and van der Waals forces, as well as aurophilic and weak $\pi-\pi$ and $\pi-H$ interactions. Thus, which isomer is formed depends on the number of solvent molecules cocrystallized. As noticed in the previous Section, all these neutral species are ionized in solution and aggregate during crystallization.

All the three isomers of $Co_6C(CO)_{12}(AuPPh_3)_4$ may be viewed as composed by an anionic $[Co_6C(CO)_{12}]^{4-}$ octahedral moiety decorated by four cationic $[AuPPh_3]^+$ units. They mainly differ for the arrangement of these cationic fragments which results in different Co_6CAu_4 cores (Figure 6). Thus, in isomer **I**, Au(1) is μ_3-bridging a triangular face of the Co_6C octahedron, generating a Co_3Au tetrahedron. The other three Au atoms are capping the three Co_2Au triangular faces of this tetrahedron (Figure 6a). The resulting Co_6CAu_4 core of **I** possesses a perfect C_{3v} symmetry with the 3-fold crystallographic axis passing through the interstitial carbide and Au(1). Isomer **I** presents

dx.doi.org/10.1021/ic501346a | Inorg. Chem. 2014, 53, 9761−9770

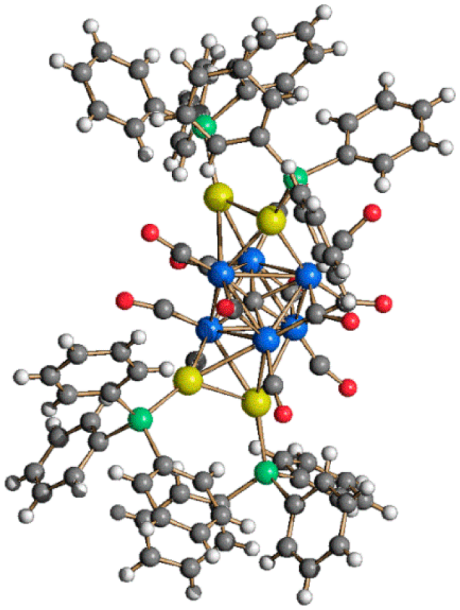

Figure 4. Molecular structure of $Co_6C(CO)_{12}(AuPPh_3)_4$ (isomer **II**) as found in $Co_6C(CO)_{12}(AuPPh_3)_4$·THF (blue, Co; yellow, Au; green, P; red, O; gray, C; white, H).

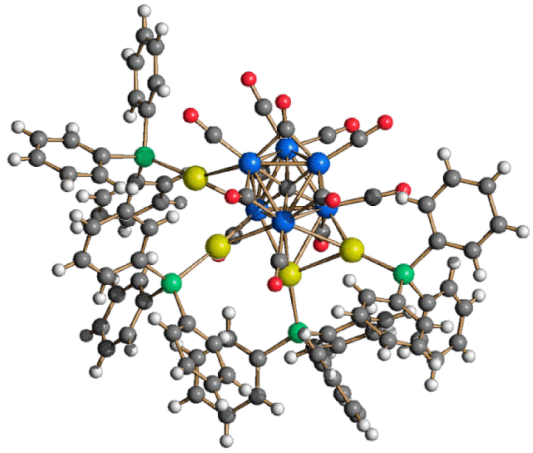

Figure 5. Molecular structure of $Co_6C(CO)_{12}(AuPPh_3)_4$ (isomer **III**) as found in $Co_6C(CO)_{12}(AuPPh_3)_4$·4THF (blue, Co; yellow, Au; green, P; red, O; gray, C; white, H).

three equivalent Au−Au bonding contacts [2.8708(12) Å] involving the central Au(1) and the three lateral Au atoms; conversely the contacts between the three lateral Au atoms are completely nonbonding [4.669(2) Å]. The cluster contains nine Co−Au bonds [2.6087(11)−2.7902(11) Å; average 2.718(3) Å]: three involving the central Au(1) [2.7902(11) Å] and two per each lateral Au atom [2.6087(11) and 2.7546(12) Å].

In the case of **II**, Au(1) is μ_3-bridging the Co(1)−Co(2)−Co(3) triangular face of the Co_6C octahedron and Au(2) caps one triangular face of the resulting tetrahedron as in **I** (Figure 6b). Then, the other two Au atoms are μ-coordinated to two Co−Co edges [Co(4)−Co(5) and Co(4)−Co(6)] of the opposite triangular Co_3-face of the octahedron, generating a Co_3Au_2 square pyramid [Co(4) apex, Au(3)−Au(4)−Co(5)−Co(6) base]. The Co_6CAu_4 core of **II** possesses idealized C_s symmetry, with the mirror plane passing through Au(1), Au(2), the interstitial C(1) carbide and Co(4). As a result, the four Au-atoms are grouped into two isolated Au_2-dimers on opposite sides of the octahedron presenting very similar Au−Au bonding contacts [Au(1)−Au(2) 2.839(3) Å; Au(3)−Au(4) 2.844(3) Å]. The Au(1)−Au(2) dimer displays five Co−Au bonds, and the Au(3)−Au(4) dimer displays four Co−Au bonds.

In the case of isomer **III**, three Au-atoms show the same coordination as in **I** (Figure 6c). Thus, Au(1) is μ_3-bridging the Co(1)−Co(2)−Co(3) triangular face of the Co_6C octahedron, whereas Au(2) and Au(3) are capping two Co_2Au faces of the resulting Co_3Au tetrahedron. Then, Au(4) is bonded to Au(2), Co(2) (which belongs to the Au-capped Co_3 face of the octahedron), and Co(4) (which belongs to the opposite Co_3 face). Overall, the Co_6CAu_4 core of **III** possesses C_1 symmetry. The cluster displays three Au−Au bonding contacts [Au(1)−Au(2) 2.9338(16) Å, Au(1)−Au(3) 2.8357(15)Å, Au(2)−Au(4) 2.8975(16) Å] and nine Co−Au bonds [2.596(3)−2.869(4) Å; average 2.713(11) Å]. It must be remarked that, despite the different structures, all isomers contain nine Co−Au bonds with very similar bonding parameters (Table 1).

The $[Co_6C(CO)_{12}]^{4-}$ fragment in the three isomers displays the same C-centered octahedral structure with very similar Co−Co and Co−$C_{carbide}$ bonding contacts (Table 1 and Figure 7). Conversely, the stereochemistry of the 12 CO ligands is sensibly different. Thus, the more symmetric isomer **I** contains 9 terminal and 3 edge bridging carbonyls, whereas both isomer **II** and **III** contain 8 terminal and 4 edge bridging CO ligands, even if distributed differently around the octahedron. Moreover, the CO ligands show some weak Au···C contacts, that are well above the sum of the covalent radii of Au and C (2.04 Å) but still below the sum of their van der Waals radii (3.36 Å).[27] In particular, **I** contains six Au···C(O) contacts in the range 2.771(5)−2.850(5) Å, **II** eight Au···C(O) contacts in the range 2.73(4)−2.96(6) Å, and **III** five Au···C(O) contacts in the range 2.75(3)−2.92(3) Å.

The free $[Co_6C(CO)_{12}]^{4-}$ cluster is not known, but the closely related paramagnetic $[Co_6C(CO)_{12}]^{3-}$ species has been recently reported.[8] It is noticeable that it shows values for the Co−Co [2.4882(14)−2.820(2) Å; average 2.654(8)Å] and Co−$C_{carbide}$ [1.8795(11)−1.8805(11)Å; average 1.880(4)Å] interactions very similar to **I**−**III**, but a different stereochemistry of the CO ligands (six terminal and six edge bridging). The change in the stereochemistry of the carbonyl ligands is due to the necessity in **I**−**III** to coordinate the four $[AuPPh_3]^+$ fragments, whereas the

Table 1. Comparison of the Most Relevant Bond Lengths (Å) in the Three Isomers of $Co_6C(CO)_{12}(AuPPh_3)_4$ as Found in $Co_6C(CO)_{12}(AuPPh_3)_4$ (I), $Co_6C(CO)_{12}(AuPPh_3)_4$·THF (II), and $Co_6C(CO)_{12}(AuPPh_3)_4$·4THF (III)

	I	II	III
Co−Co	2.5108(12)−2.7816(16) average 2.652(5)	2.447(10)−2.807(8) average 2.65(3)	2.500(5)−2.910(5) average 2.653(17)
Co−$C_{carbide}$	1.856(3)−1.901(4) average 1.878(9)	1.75(4)−2.00(4) average 1.88(9)	1.85(3)−1.91(2) average 1.88(5)
Co−Au	2.6087(11)−2.7902(11) average 2.718(3)	2.588(7)−2.764(7) average 2.70(2)	2.596(3)−2.869(4) average 2.713(11)
Au−P	2.2874(14)−2.326(2) average 2.297(3)	2.260(13)−2.301(14) average 2.28(3)	2.289(7)−2.311(7) average 2.299(14)
Au−Au	2.8708(12)	2.839(3)−2.844(3) average 2.84(2)	2.8357(15)−2.9338(15) average 2.889(3)

dx.doi.org/10.1021/ic501346a | Inorg. Chem. 2014, 53, 9761−9770

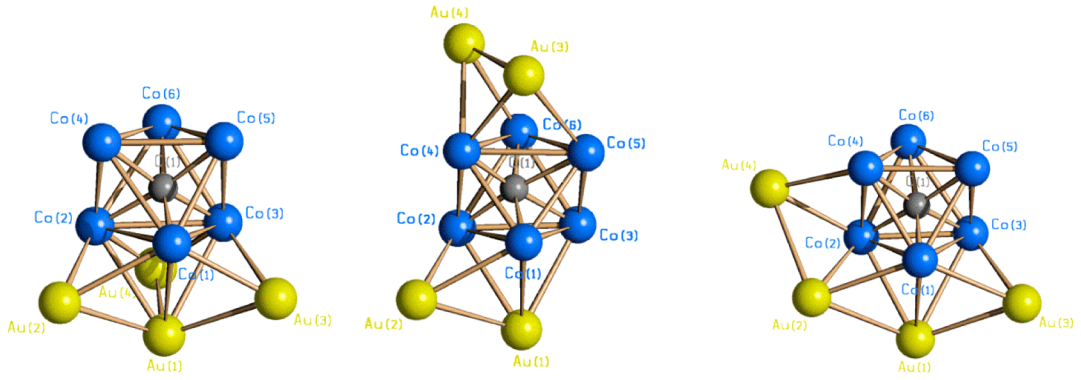

Figure 6. Co_6CAu_4 cores of (a) isomer **I**, (b) isomer **II**, and (c) isomer **III** of $Co_6C(CO)_{12}(AuPPh_3)_4$.

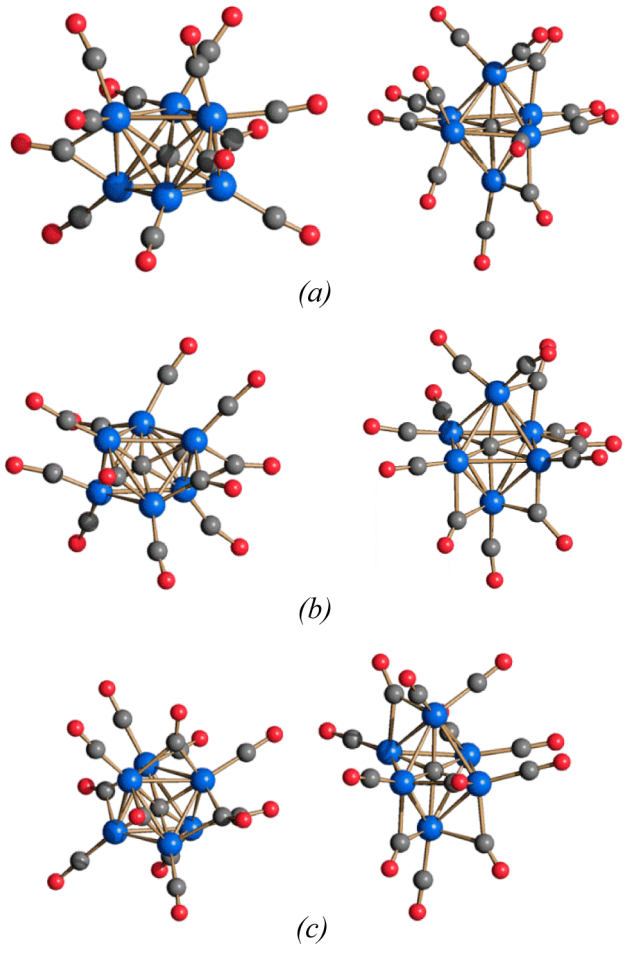

Figure 7. $[Co_6C(CO)_{12}]^{4-}$ fragment of (a) isomer **I**, (b) isomer **II** and (c) isomer **III** of $Co_6C(CO)_{12}(AuPPh_3)_4$. Two views are reported per each isomer, one similar to Figures 3–6 and the second one to better appreciate its octahedral structure.

Co_6C core seems rather robust since its bonding parameters do not change appreciably upon coordination of the Au(I) fragments.

Overall, the three isomers of $Co_6C(CO)_{12}(AuPPh_3)_4$ display very similar bonding parameters (number of bonds and distances) when the stronger Co–Co, Co–$C_{carbide}$, Co–Au, and Au–P interactions are considered. The differences are mainly focused on the weaker Au–Au and Au···C(O) interactions, as well as the stereochemistry of the carbonyls and, above all, the spatial arrangement of the four $[AuPPh_3]^+$ fragments. We might expect that these isomers have very similar internal energies, and thus, small differences in the van der Waals forces due to the interactions with a variable amount of cocrystallized solvent molecules cause the formation in the solid state of **I**, **II**, or **III**. At the same time, it seems that the different coordination modes of the four $[AuPPh_3]^+$ fragments do not influence very much the bonding in the $[Co_6C(CO_{12}]^{4-}$ core.

2.3. Crystal Structure of $Co_6C(CO)_{12}(PPh_3)(AuPPh_3)_2$ as found in $Co_6C(CO)_{12}(PPh_3)(AuPPh_3)_2$·toluene (IV) and $Co_6C(CO)_{12}(PPh_3)(AuPPh_3)_2$·0.5toluene (V). The molecular structure of $Co_6C(CO)_{12}(PPh_3)(AuPPh_3)_2$ has been determined as its $Co_6C(CO)_{12}(PPh_3)(AuPPh_3)_2$·toluene (**IV**) and $Co_6C(CO)_{12}(PPh_3)(AuPPh_3)_2$·0.5toluene (**V**) solvates (Figure 8 and Table 2). The neutral cluster shows some differences in the two solvates, even if more limited than in the case of $Co_6C(CO)_{12}(AuPPh_3)_4$. In this Section, the structure of $Co_6C(CO)_{12}(PPh_3)(AuPPh_3)_2$ will be also compared to the homoleptic analogous $Co_6C(CO)_{13}(AuPPh_3)_2$, previously reported in the literature.[26]

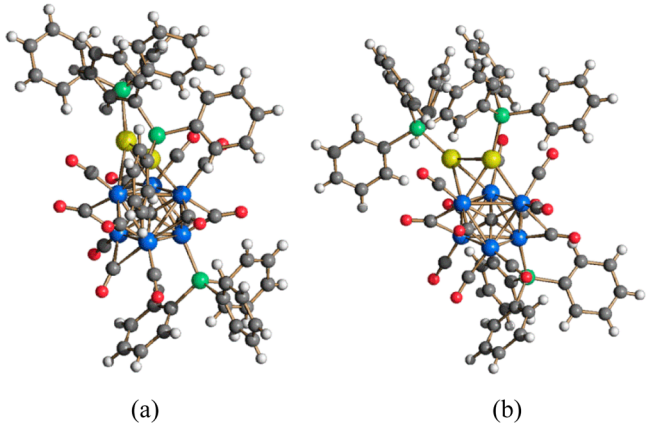

Figure 8. Molecular structure of $Co_6C(CO)_{12}(PPh_3)(AuPPh_3)_2$ as found in (a) $Co_6C(CO)_{12}(PPh_3)(AuPPh_3)_2$·toluene (**IV**) and (b) $Co_6C(CO)_{12}(PPh_3)(AuPPh_3)_2$·0.5toluene (**V**) (blue, Co; yellow, Au; green, P; red, O; gray, C; white, H).

The structure of $Co_6C(CO)_{12}(PPh_3)(AuPPh_3)_2$ in both solvates may be described as composed by an octahedral

dx.doi.org/10.1021/ic501346a | Inorg. Chem. 2014, 53, 9761–9770

Table 2. Most Relevant Bond Lengths (Å) of $Co_6C(CO)_{12}(PPh_3)(AuPPh_3)_2$ as Found in $Co_6C(CO)_{12}(PPh_3)(AuPPh_3)_2$·toluene (IV) and $Co_6C(CO)_{12}(PPh_3)(AuPPh_3)_2$·0.5toluene (V) Compared to $Co_6C(CO)_{13}(AuPPh_3)_2$[26]

	IV	V	$Co_6C(CO)_{13}(AuPPh_3)_2$[a]
Co−Co	2.498(2)−2.826(2) average 2.642(7)	2.501(2)−2.833(2) average 2.641(7)	2.493(7)−2.992(7) average 2.65(2)
$Co-C_{carbide}$	1.838(10)−1.911(10) average 1.87(2)	1.828(11)−1.924(11) average 1.87(3)	1.83(4)−1.98(5) average 1.87(12)
Co−Au	2.6020(15)−2.6709(16) average 2.646(3)	2.6015(15)−2.6704(16) average 2.648(3)	2.641(5)−2.848(5) average 2.740(11)
Au−P	2.289(3)−2.300(3) average 2.294(4)	2.284(3)−2.288(3) average 2.286(4)	2.310(17)−2.318(13) average 2.31(2)
Au−Au	2.9194(7)	2.8745(9)	2.842(2)

[a]See ref 26.

$[Co_6C(CO)_{12}(PPh_3)]^{2-}$ core decorated by two $[AuPPh_3]^+$ fragments. These are μ-coordinated to two adjacent Co−Co edges of the octahedron (Figure 9), resembling the coordination

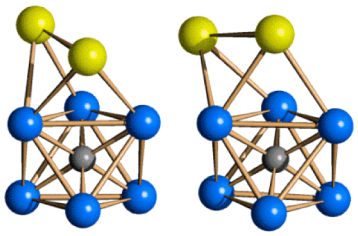

Figure 9. Co_6CAu_2 cores of $Co_6C(CO)_{12}(PPh_3)(AuPPh_3)_2$ as found in (a) $Co_6C(CO)_{12}(PPh_3)(AuPPh_3)_2$·toluene (**IV**) and (b) $Co_6C(CO)_{12}(PPh_3)(AuPPh_3)_2$·0.5toluene (**V**) (blue, Co; yellow, Au; green, P; red, O; gray, C; white, H).

of the top $[AuPPh_3]^+$ fragments of **II** (Figure 6b, top). This results in the formation of four Co−Au bonds in **IV** and **V** with very similar bonding parameters (Table 2). Also the Co−Co and $Co-C_{carbide}$ distances of the $[Co_6C(CO)_{12}(PPh_3)]^{2-}$ core are almost identical in **IV** and **V**.

The most significant differences between **IV** and **V** concern the Au−Au interaction and the stereochemistry of the CO ligands. The Au−Au bonding distance is significantly longer in **IV** [2.9194(7) Å] than **V** [2.8745(9)Å]. Moreover, **IV** contains six terminal and six edge bridging carbonyls, whereas **V** possesses seven terminal and five edge bridging CO ligands (Figure 10). One PPh_3 ligand is, in both cases, bonded to a Co atom on the triangular face of the octahedron not bonded to any Au atom. In addition, both clusters show four weak Au···C(O) contacts [2.769(12)-2.879(14) Å in **IV**; 2.753(14)-2.838(12) Åin **V**].

IV and **V** may be compared to the homoleptic $Co_6C(CO)_{13}(AuPPh_3)_2$ cluster previously reported in the literature,[26] that displays a different coordination mode of the $[AuPPh_3]^+$ fragments to the octahedral $[Co_6C(CO)_{13}]^{2-}$ core compared to **IV** and **V**. Thus, one Au is μ_3-coordinated to a Co_3 face of the octahedron, whereas the second Au is capping one Co_2Au face of the resulting Co_3Au tetrahedron, resembling the coordination of the bottom $[AuPPh_3]^+$ fragments of **II** (Figure 6b, bottom). Overall, $Co_6C(CO)_{13}(AuPPh_3)_2$ contains five Co−Au bonds, whereas only four are present in **IV** and **V**. The different coordination of the Au(I) fragments determines also a different stereochemistry of the CO ligands, since $Co_6C(CO)_{13}(AuPPh_3)_2$ displays nine terminal and four edge bridging CO's. The Au−Au bonds in the homoleptic cluster [2.842(2) Å] is sensibly shorter than in **IV** and **V**.

2.4. Theoretical Investigation. To shed some light on the isomers **I**, **II**, and **III** found in the solid state, a series of DFT optimization were performed using the B97D functional[28] with

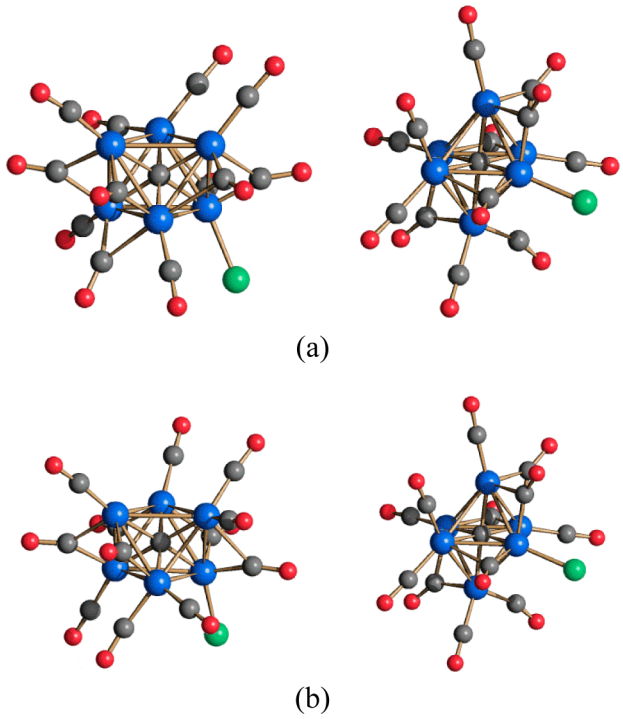

Figure 10. $[Co_6C(CO)_{13}]^{2-}$ fragment of $Co_6C(CO)_{12}(PPh_3)(AuPPh_3)_2$ as found in (a) $Co_6C(CO)_{12}(PPh_3)(AuPPh_3)_2$·toluene (**IV**) and (b) $Co_6C(CO)_{12}(PPh_3)(AuPPh_3)_2$·0.5toluene (**V**). Two views are reported per each isomer, one similar to Figure 8 and the second one to betterappreciate its octahedral structure.

the inclusion of the dispersion forces. These in principle could help to reproduce the different stability of the isomers. In the first attempts we used simplified models starting from the crystallographic coordinates with PH_3 in place of PPh_3 and by neglecting the cocrystallized molecules. Although this kind of approach gave satisfactory results in the previous investigation of the $Ni_6C(CO)_9(AuPPh_3)_4$ cluster,[19] it appears insufficient in the present case. In fact, during the optimizations the $AuPH_3$ fragments move away from the original positions and the obtained models were unsatisfactory. In the second series of calculations, we decided to include in the models also the phenyl rings. The general features of the models were conserved but it was impossible to obtain the convergence for isomers **I** and **II**, likely imputed to the complex nature of these molecules. Nevertheless some useful information from the calculations could be obtained. First of all, qualitative single point calculations on the crystallographic structures revealed that **I** is 14 and 2.5 kcal/mol more stable than **II** and **III**, respectively. The energy differences are reasonably small and existence of the isomers in the crystals is consistent with solid-state packing effects, neglected during the modeling of a single isolated molecule.

dx.doi.org/10.1021/ic501346a | Inorg. Chem. 2014, 53, 9761−9770

More intriguing fact is the incapacity of the PH_3 models in simulating the experimental structures. We can conclude that the aurophilic interactions alone are not able to stabilize the models. The $\pi-\pi$ and $\pi-H$ interactions have also a stabilizing role in the clusters. In particular the number of such interactions and the stability of the clusters seem to be correlated and they change in the same order (**I** ≅ **III** > **II**). In any case, for the isomer **III** we were able to complete the geometry optimization of the whole compound and a comparison between the optimized and the experimental structures is pointed out in Table 3. The Co_6-C core is satisfactorily reproduced except for a slight overestimation mainly attributable to the usage of the pseudopotential, especially for the two equatorial Co centers with a bridging Au atom (3.05 vs. the experimental value of 2.83 Å). An opposite trend may be pointed out for the Au−Au distances, being two of them shorter than the X-ray ones (2.84 vs crystallographic 2.93 and 2.90 Å). The main discrepancy concerns the Co−Au bonding pattern, since only eight rather than nine (in the X-ray structure) Co−Au bonding distances have been predicted by the optimization, being the Au_1-Co_3 significantly elongated (0.4 Å).

Table 3. Comparison of the Most Relevant Bond Lengths (Å) between the $Co_6C(CO)_{12}(AuPPh_3)_4$·4THF (III) and the Calculated Structure

	$Co_6C(CO)_{12}(AuPPh_3)_4$·4THF (III)	calculated III
Co−Co	2.500(5)−2.911(5) average 2.653(17)	2.512−3.054 average 2.688
$Co-C_{carbide}$	1.85(3)−1.91(2) average 1.88(5)	1.879−1.949 average 1.910
Co−Au	2.597(3)−2.869(4) average 2.714(11)	2.639−2.977 average 2.802
Au−P	2.289(7)−2.310(7) average 2.299(14)	2.319−2.324 average 2.320
Au−Au	2.8358(15)−2.9336(15) average 2.889(3)	2.842−2.860 average 2.852

The gap between the highest occupied molecular orbital (HOMO, Figure 11a) and the lowest unoccupied one (LUMO, Figure 11b) was estimated to be 1.29 eV. In contrast with the precedent case of $Ni_6(C)Au_4$ cluster,[19] where the HOMO had a strong Ni character while the LUMO was mainly localized on the Au, in the present case both HOMO and the LUMO are largely located on the Co atoms rather than on the Au (69.6 and 60.7 vs 8.04 and 11.3% for HOMO and LUMO, respectively). Only in the LUMO+2 (see Figure 11c), +0.38 eV higher in energy than the LUMO, the contribution from the gold is only slightly bigger than the Co one (32.3 vs 29.7).

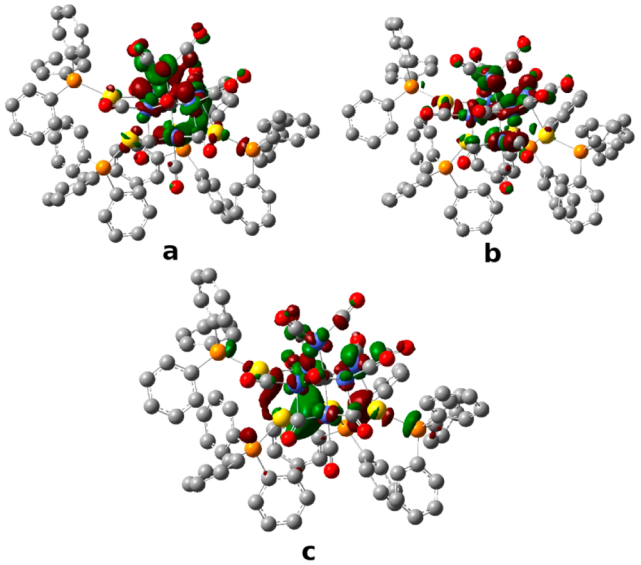

Figure 11. Graphical plots (isosurface = 0.03) of the (a) HOMO, (b) LUMO, and (c) LUMO+2 of $Co_6C(CO)_{12}(AuPPh_3)_4$.

3. CONCLUSIONS

Two new 86 CVE octahedral Co-carbide carbonyl clusters decorated by $[AuPPh_3]^+$ fragments have been herein described, namely, $Co_6C(CO)_{12}(AuPPh_3)_4$ and $Co_6C(CO)_{12}(PPh_3)(AuPPh_3)_2$. The former displays three different isomers **I**−**III** in the solid state, which contain the same $[Co_6C(CO)_{12}]^{4-}$ core and show a different arrangement of the Au(I) fragments. The different structure of isomers **I**−**III** is a consequence of the different number of cocrystallized THF molecules (0, 1, and 4, respectively). Theoretical investigations suggest that the formation in the solid state of the three isomers during crystallization is governed by packing and van der Waals forces, as well as aurophilic and weak $\pi-\pi$ and $\pi-H$ interactions. A significant, even if minor, effect of the cocrystallized solvent molecules on the structure of the cluster has been observed also in the case of $Co_6C(CO)_{12}(PPh_3)(AuPPh_3)_2$.

Comparing the bonding parameters of **I**−**III** and **IV**−**V**, it is noteworthy that the Co−Co and $Co-C_{carbide}$ distances are almost the same in all the clusters, whereas significant differences involve the Co−Au and Au−Au distances. This suggests that their Co_6C cores are rigid and not very much affected by the ligands and fragments which decorate their surfaces. As a result, these Co_6C clusters decorated by Au-fragments are very good platforms to test aurophilicity and other weak forces, since their different energies are dictated only by the weak interactions on the surfaces, whereas the stronger core-interactions are almost constant. At the same time, this explains why different isomers are formed in the solid state as the consequence of a different solvation of the solid and packing forces.

4. EXPERIMENTAL SECTION

4.1. General Procedures. All reactions and sample manipulations were carried out using standard Schlenk techniques under nitrogen and in dried solvents. All the reagents were commercial products (Aldrich) of the highest purity available and used as received, except $[NMe_3(CH_2Ph)]_2[Co_6C(CO)_{15}]$, $[NEt_4]_2[Co_6C(CO)_{15}]$,[5] $[NMe_3(CH_2Ph)]_2[Co_8C(CO)_{18}]$,[7] and $Au(PPh_3)Cl$,[29] which were prepared according to the literature. Analysis of Co and Au were performed by atomic absorption on a Pye-Unicam instrument. Analyses of C, H, and N were obtained with a Thermo Quest Flash EA 1112NC instrument. IR spectra were recorded on a PerkinElmer Spectrum One interferometer in CaF_2 cells. $^{31}P\{^1H\}$ NMR measurements were performed on a Varian Mercury Plus 400 MHz instrument. The phosphorus chemical shifts were referenced to external H_3PO_4 (85% in D_2O). Structure drawings have been performed with SCHAKAL99.[30]

4.2. Synthesis of $Co_6C(CO)_{12}(AuPPh_3)_4$ (I−III). $Au(PPh_3)Cl$ (1.41 g, 2.82 mmol) was added as a solid to a solution of $[NMe_3(CH_2Ph)]_2[Co_6C(CO)_{15}]$ (1.02 g, 0.94 mmol) in THF (30 mL) over a period of 2 h. The resulting mixture was further stirred at room temperature for 4 h, and then, the solvent was removed *in vacuo*. The residue was washed with water (40 mL) and extracted with THF (20 mL). A crystalline material was obtained by layering *n*-hexane (40 mL) on the THF solution (yield 0.2−0.4 g). This solid may contain one or a mixture of the three solvate crystals $Co_6C(CO)_{12}(AuPPh_3)_4$ (**I**), $Co_6C(CO)_{12}(AuPPh_3)_4$·THF (**II**), or $Co_6C(CO)_{12}(AuPPh_3)_4$·4THF (**III**). The different content of cocrystallized THF makes meaningless elemental analyses or the determination of the yield.

dx.doi.org/10.1021/ic501346a | *Inorg. Chem.* 2014, 53, 9761−9770

Table 4. Crystal Data and Experimental Details for $Co_6C(CO)_{12}(AuPPh_3)_4$ (I), $Co_6C(CO)_{12}(AuPPh_3)_4$·THF (II), $Co_6C(CO)_{12}(AuPPh_3)_4$·4THF (III), $Co_6C(CO)_{12}(PPh_3)(AuPPh_3)_2$·toluene (IV), and $Co_6C(CO)_{12}(PPh_3)(AuPPh_3)_2$·0.5toluene (V)

	I	II	III
formula	$C_{85}H_{60}Au_4Co_6O_{12}P_4$	$C_{89}H_{68}Au_4Co_6O_{13}P_4$	$C_{101}H_{92}Au_4Co_6O_{16}P_4$
Fw	2538.66	2610.76	2827.07
T, K	295(2)	293(2)	100(2)
λ, Å	0.710 73	0.710 73	0.710 73
crystal system	rhombohedral	monoclinic	monoclinic
space group	$R\bar{3}$	$P2_1/n$	$P2_1/c$
a, Å	22.678(11)	14.229(3)	14.581(4)
b, Å	22.678(11)	14.397(3)	13.802(4)
c, Å	27.587(13)	42.721(8)	48.590(13)
β, deg	90	90.652(2)	97.902(3)
cell volume, Å^3	12287(10)	8751(3)	9685(4)
Z	6	4	4
D_c, g cm^{-3}	2.059	1.982	1.939
μ, mm^{-1}	8.453	7.916	7.163
$F(000)$	7224	4976	5456
crystal size, mm	0.21 × 0.18 × 0.12	0.16 × 0.12 × 0.11	0.15 × 0.13 × 0.10
θ limits, deg	1.27−26.00	1.49−22.00	1.41−25.03
index ranges	$-27 \le h \le 27$	$-14 \le h \le 14$	$-17 \le h \le 17$
	$-27 \le k \le 27$	$-15 \le k \le 15$	$-16 \le k \le 16$
	$-33 \le l \le 34$	$-45 \le l \le 45$	$-57 \le l \le 57$
reflections collected	42 591	59 475	82 110
independent reflections	5378 [R_{int} = 0.0433]	10 698 [R_{int} = 0.3096]	16 633 [R_{int} = 0.0990]
completeness to θ max	100.0%	99.8%	97.1%
data/restraints/parameters	5378/180/334	10 698/580/877	16 633/346/1068
goodness of fit on F^2	1.076	1.123	1.188
R_1 ($I > 2\sigma(I)$)	0.0247	0.1253	0.1246
wR_2 (all data)	0.0666	0.3134	0.2750
largest diff. peak and hole, e Å^{-3}	1.634/−0.693	2.009/−1.114	7.626/−5.806

	IV	V
formula	$C_{74}H_{53}Au_2Co_6O_{12}P_3$	$C_{70.5}H_{49}Au_2Co_6O_{12}P_3$
Fw	1974.59	1928.52
T, K	294(2)	100(2)
λ, Å	0.710 73	0.710 73
crystal system	monoclinic	triclinic
space group	$P2_1/c$	$P\bar{1}$
a, Å	11.0288(7)	11.009(4)
b, Å	21.2558(13)	13.736(5)
c, Å	30.3199(19)	23.556(8)
α, deg	90	90.154(4)
β, deg	99.9190(10)	93.606(4)
γ, deg	90	110.442(4)
cell volume, Å^3	7001.5(8)	3330.2(19)
Z	4	2
D_c, g cm^{-3}	1.873	1.923
μ, mm^{-1}	5.688	5.977
$F(000)$	3832	1866
crystal size, mm	0.14 × 0.12 × 0.10	0.18 × 0.16 × 0.14
θ limits, deg	1.36−25.03	1.58−26.00
index ranges	$-13 \le h \le 13$	$-13 \le h \le 13$
	$-25 \le k \le 25$	$-16 \le k \le 16$
	$-36 \le l \le 36$	$-29 \le l \le 29$
reflections collected	66 775	33 698
independent reflections	12 356 [R_{int} = 0.1462]	12 995 [R_{int} = 0.0911]
completeness to θ max	99.9%	99.2%
data/restraints/parameters	12 356/404/719	12 995/464/858
goodness on fit on F^2	0.994	0.993
R_1 ($I > 2\sigma(I)$)	0.0608	0.0600
wR_2 (all data)	0.1285	0.1491
largest diff. peak and hole, e Å^{-3}	0.951/−0.821	3.291/−1.865

dx.doi.org/10.1021/ic501346a | Inorg. Chem. 2014, 53, 9761−9770

IR (nujol, 293 K) ν(CO): $Co_6C(CO)_{12}(AuPPh_3)_4$ (**I**) 2034(s), 2004(vs), 1966(s), 1921(vs), 1879(sh), and 1799(vs) cm^{-1}; $Co_6C(CO)_{12}(AuPPh_3)_4$·THF (**II**) 2009(vs), 19810(s), 1941(m), 1834(m), and 1812(m) cm^{-1}; $Co_6C(CO)_{12}(AuPPh_3)_4$·4THF (**III**) 2022(m), 2008(m), 1965(s), 1939(w), 1875(w), 1857(w), 1834(w), 1821(m), and 1796(w) cm^{-1}.

4.3. Synthesis of $Co_6C(CO)_{12}(PPh_3)(AuPPh_3)_2$·toluene (IV). $Au(PPh_3)Cl$ (0.155 g, 0.310 mmol) was added as a solid to a solution of $[NEt_4]_2[Co_6C(CO)_{15}]$ (0.325 g, 0.310 mmol) in CH_2Cl_2 (20 mL) at −12 °C and was stirred at this temperature for 1 h. Then, the solution was allowed to reach room temperature before adding $AgNO_3$ (0.053 g, 0.311 mmol) and PPh_3 (0.163 g, 0.622 mmol) as solids. The resulting mixture was further stirred at room temperature for 2 h, and then, the solvent was removed *in vacuo*. The residue was washed with water (40 mL) and extracted with toluene (20 mL). Crystals of $Co_6C(CO)_{12}(PPh_3)(AuPPh_3)_2$·toluene (**IV**) suitable for X-ray analyses were obtained by layering *n*-hexane (40 mL) on the toluene solution. **IV** is formed as a side product in mixture with other amorphous products, not yet identified, which represent the major product. A few crystals of **IV** were mechanically separated from the amorphous solid and used for X-ray crystallography. No further analyses were possible. IR (nujol, 293 K) ν(CO): 2041(m), 1999(s), 1984(sh), 1953(s), 1856(m), and 1830(m) cm^{-1}.

4.4. Synthesis of $Co_6C(CO)_{12}(PPh_3)(AuPPh_3)_2$·0.5toluene (V). $Au(PPh_3)Cl$ (0.765 g, 1.53 mmol) was added as solid to a solution of $[NMe_3(CH_2Ph)]_2[Co_8C(CO)_{18}]$ (0.66 g, 0.51 mmol) in acetone (20 mL) over a period of 2 h. The resulting mixture was further stirred at room temperature for 48 h, and then, the solvent was removed *in vacuo*. The residue was washed with water (40 mL) and extracted with toluene (20 mL). Crystals of $Co_6C(CO)_{12}(PPh_3)(AuPPh_3)_2$·0.5toluene (**V**) suitable for X-ray analyses were obtained by layering *n*-hexane (40 mL) on the toluene solution (yield 0.29 g, 22% based on Co, 20% based on Au).

$C_{70.5}H_{49}Au_2Co_6O_{12}P_3$ (1928.52): Anal. calcd. C 43.91, H 2.56, Au 20.43, Co18.33; found: C 44.11, H 2.85, Au 20.13, Co18.05%. IR (nujol, 293 K) ν(CO): 2056(w), 2035(w), 1997(vs), 1980(sh), 1953(s), 1859(w), 1829(m), and 1801(sh) cm^{-1}. IR (toluene, 293 K) ν(CO): 2059(w), 2008(s), 1958(w), and 1848(w) cm^{-1}.

4.5. X-ray Crystallographic Study. Crystal data and collection details for $Co_6C(CO)_{12}(AuPPh_3)_4$ (**I**), $Co_6C(CO)_{12}(AuPPh_3)_4$·THF (**II**), $Co_6C(CO)_{12}(AuPPh_3)_4$·4THF (**III**), $Co_6C(CO)_{12}(PPh_3)(AuPPh_3)_2$·toluene (**IV**), and $Co_6C(CO)_{12}(PPh_3)(AuPPh_3)_2$·0.5toluene (**V**) are reported in Table 4. The diffraction experiments were carried out on a Bruker APEX II diffractometer equipped with a CCD detector using Mo Kα radiation. Data were corrected for Lorentz polarization and absorption effects (empirical absorption correction SADABS).[31] Structures were solved by direct methods and refined by full-matrix least-squares based on all data using F^2.[32] Hydrogen atoms were fixed at calculated positions and refined by a riding model. All non-hydrogen atoms in the cluster molecules were refined with anisotropic displacement parameters, whereas solvent molecules were treated isotropically.

$Co_6C(CO)_{12}(AuPPh_3)_4$ (I). The asymmetric unit of the unit cell contains one-third of a cluster with Au(1), P(1), and C(1) located on a 3-axis. Similar *U* restraints (s.u. 0.01) were applied to the C and O atoms.

$Co_6C(CO)_{12}(AuPPh_3)_4$·THF (II). The asymmetric unit of the unit cell contains one cluster and one THF molecule (all located on general positions). Similar *U* restraints (s.u. 0.005) were applied to CO and Ph groups. Some C and O atoms were restrained to isotropic behavior (ISOR line in SHELXL, s.u. 0.005). Restraints to bond distances were applied as follow (s.u. 0.01): 1.43 Å for C−O and 1.53 Å for C−C in THF. The Ph rings were constrained to fit regular hexagons (AFIX 66 line in SHELXL). The compound gives rise to very small and low-quality crystals, and therefore, the data were cut at $2\theta = 44°$.

$Co_6C(CO)_{12}(AuPPh_3)_4$·4THF (III). The asymmetric unit of the unit cell contains one cluster and four THF molecules (all located on general positions). Similar *U* restraints (s.u. 0.02) were applied to the THF molecules. Restraints to bond distances were applied as follow (s.u. 0.02): 1.43 Å for C−O and 1.53 Å for C−C in THF. Some C and O atoms were restrained to isotropic behavior (ISOR line in SHELXL, s.u. 0.02). The Ph rings were constrained to fit regular hexagons (AFIX 66 line in SHELXL). Some residual large electron densities remain after refinement, mainly due to absorption effects, which were not fully corrected in view of the presence of several heavy atoms in a very irregularly shaped crystal.

$Co_6C(CO)_{12}(PPh_3)(AuPPh_3)_2$·toluene (IV). The asymmetric unit of the unit cell contains one cluster and one toluene molecule (all located on general positions). Similar *U* restraints (s.u. 0.005) were applied to the C and O atoms. The Ph rings were constrained to fit regular hexagons (AFIX 66 line in SHELXL). Restraints to bond distances were applied as follows (s.u. 0.01): 1.51 Å for $C(sp^3)$−$C(sp^2)$ in toluene.

$Co_6C(CO)_{12}(PPh_3)(AuPPh_3)_2$·0.5toluene (V). The asymmetric unit of the unit cell contains one cluster molecule (located on a general position) and one-half of a toluene molecule disordered over two equally populated symmetry related (by an inversion center) positions. Similar *U* restraints (s.u. 0.005) were applied to the C atoms. Restraints to bond distances were applied as follows (s.u. 0.01): 1.51 Å for $C(sp^3)$−$C(sp^2)$ in toluene.

COMPUTATIONAL DETAILS

The single-point and optimization calculations were carried out at the B97D-DFT level of theory within the Gaussian 09 package.[33] The effective Stuttgart−Dresden core potential[34] was adopted for the Co and Au atoms, while for the remaining atomic species, the basis set used was 6-31G with the important addition of the polarization function (d and p) for all elements, including H atoms. The coordination of the optimized structure as well as the energy are reported in the Supporting Information. The calculations of the single atom contribution to the frontier molecular orbitals were performed on the optimized structure within AOMIX package.[35]

ASSOCIATED CONTENT

Supporting Information

CIF files giving X-ray crystallographic data for the structure determination of $Co_6C(CO)_{12}(AuPPh_3)_4$ (**I**), $Co_6C(CO)_{12}(AuPPh_3)_4$·THF (**II**), $Co_6C(CO)_{12}(AuPPh_3)_4$·4THF (**III**), $Co_6C(CO)_{12}(PPh_3)(AuPPh_3)_2$·toluene (**IV**), and $Co_6C(CO)_{12}(PPh_3)(AuPPh_3)_2$·0.5toluene (**V**). The coordinates of the optimized structure of **III**. This material is available free of charge via the Internet at http://pubs.acs.org.

AUTHOR INFORMATION

Corresponding Author

*E-mail: stefano.zacchini@unibo.it.

Notes

The authors declare no competing financial interest.

ACKNOWLEDGMENTS

Funding by Fondazione CARIPLO, Project No. 2011-0289, is heartily acknowledged. The University of Bologna is acknowledged for financial support to this work (FARB - Linea d'Intervento 2, "Catalytic transformation of biomass-derived materials into high added-value chemicals", 2014−2016). A.I. and G.M. acknowledge HP10CHEVJ8 of CINECA and CREA (Centro RicercheEnergia e Ambiente) of Colle Val d'Elsa (Siena, Italy) for computational resources.

REFERENCES

(1) (a) *The Chemistry of Metal Cluster Complexes;* Shriver, D. F., Kaesz, H. D., Adams, R. D., Eds.; VCH: New York, 1990. (b) Mingos, D. M. P.; Wales, D. J. *Introduction to Cluster Chemistry;* Prentice Hall: Englewood Cliffs, 1990. (c) Mingos, D. M. P. *Acc. Chem. Res.* **1984**, *17*, 311.

(2) (a) Halet, J.-F.; Evans, D. G.; Mingos, D. M. P. *J. Am. Chem. Soc.* **1988**, *110*, 87. (b) Wade, K. *Adv. Inorg. Chem. Radiochem.* **1976**, *18*, 1.
(3) (a) Gonzales-Moraga, G. *Cluster Chemistry;* Springer-Verlag: Berlin, Germany, 1993. (b) *Clusters and Colloids;* Schmid, G., Ed.; VCH, Weinheim, Germany, 1994. (c) *Catalysis by Di- and Polynuclear Metal Cluster Complexes;* Adams, R. D., Cotton, F. A., Eds.; Wiley-VCH: New York, 1998. (d) *Metal Clusters in Chemistry;* Braunstein, P., Oro, L. A., Raithby, P. R., Eds.; Wiley-VCH: Weinheim, Germany, 1999.
(4) (a) Zacchini, S. *Eur. J. Inorg. Chem.* **2011**, 4125. (b) Femoni, C.; Iapalucci, M. C.; Kaswalder, F.; Longoni, G.; Zacchini, S. *Coord. Chem. Rev.* **2006**, *250*, 1580.
(5) (a) Albano, V. G.; Chini, P.; Martinengo, S.; Sansoni, M.; Strumolo, D. *J. Chem. Soc., Chem. Commun.* **1974**, 299. (b) Martinengo, S.; Strumolo, D.; Chini, P.; Albano, V. G.; Braga, D. *J. Chem. Soc., Dalton Trans.* **1985**, 35.
(6) (a) Albano, V. G.; Braga, D.; Martinengo, S. *J. Chem. Soc., Dalton Trans.* **1986**, 981. (b) Albano, V. G.; Chini, P.; Ciani, G.; Sansoni, M.; Strumolo, D.; Heaton, B. T.; Martinengo, S. *J. Am. Chem. Soc.* **1976**, *98*, 5027.
(7) (a) Albano, V. G.; Chini, P.; Ciani, G.; Martinengo, S.; Sansoni, M. *J. Chem. Soc., Dalton Trans.* **1978**, 468. (b) Albano, V. G.; Chini, P.; Ciani, G.; Sansoni, M.; Martinengo, S. *J. Chem. Soc., Dalton Trans.* **1980**, 163.
(8) Ciabatti, I.; Femoni, C.; Hayatifar, M.; Iapalucci, M. C.; Longoni, G.; Pinzino, C.; Solmi, M. V.; Zacchini, S. *Inorg. Chem.* **2014**, *53*, 3818.
(9) (a) Ciabatti, I.; Femoni, C.; Iapalucci, M. C.; Longoni, G.; Zacchini, S. *J. Cluster Sci.* **2014**, *25*, 115. (b) Femoni, C.; Kaswalder, F.; Iapalucci, M. C.; Longoni, G.; Zacchini, S. *Chem. Commun.* **2006**, 2135. (c) Femoni, C.; Iapalucci, M. C.; Longoni, G.; Ranuzzi, F.; Zacchini, S.; Fedi, S.; Zanello, P. *Eur. J. Inorg. Chem.* **2007**, 4064.
(10) (a) Demartin, F.; Iapalucci, M. C.; Longoni, G. *Inorg. Chem.* **1993**, *32*, 5536. (b) Ciabatti, I.; Femoni, C.; Iapalucci, M. C.; Longoni, G.; Zacchini, S.; Zarra, S. *Nanoscale* **2012**, *4*, 4166. (c) Bernardi, A.; Femoni, C.; Iapalucci, M. C.; Longoni, G.; Ranuzzi, F.; Zacchini, S.; Zanello, P.; Fedi, S. *Chem.—Eur. J.* **2008**, *14*, 1924. (d) Imhof, D.; Venanzi, L. M. *Chem. Soc. Rev.* **1994**, 185.
(11) (a) Raithby, P. R. *Platinum Met. Rev.* **1998**, *42*, 146. (b) Ciabatti, I.; Femoni, C.; Iapalucci, M. C.; Longoni, G.; Zacchini, S.; Fedi, S.; Fabrizi de Biani, F. *Inorg. Chem.* **2012**, *51*, 11753. (c) Lauher, J. W.; Wald, K. *J. Am. Chem. Soc.* **1981**, *103*, 7648.
(12) (a) Zank, J.; Schier, A.; Schmidbaur, H. *J. Chem. Soc., Dalton Trans.* **1998**, 323. (b) Albano, V. G.; Castellari, C.; Femoni, C.; Iapalucci, M. C.; Longoni, G.; Monari, M.; Rauccio, M.; Zacchini, S. *Inorg. Chim. Acta* **1999**, *291*, 372. (d) Braunstein, P.; Rosé, J.; Dusausoy, Y.; Mangeot, J.-P. *C. R. Chim.* **1982**, *294*, 967.
(13) (a) Hoffmann, R. *Angew. Chem., Int. Ed.* **1982**, *21*, 711. (b) Mingos, D. M. P. *Gold Bull.* **1984**, *17*, 5.
(14) (a) Lauher, J. W.; Wald, K. *J. Am. Chem. Soc.* **1982**, *103*, 7648. (b) Braunstein, P.; Rosé, J.; Dusausoy, Y.; Mangeot, J.-P. *C. R. Chim.* **1982**, *294*, 967. (c) Li, X.; Kiran, B.; Wang, L.-S. *J. Phys. Chem. A* **2005**, *109*, 4366.
(15) Braunstein, P.; Rosé, J. *Gold Bull.* **1985**, *18*, 17.
(16) Lewis, J.; Raithby, P. R. In *Metal Clusters in Chemistry;* Braunstein, P., Oro, L. A., Raithby, P. R., Eds.; Wiley-VCH: Weinheim, Germany, 1999; p 348.
(17) Vargas, M. D.; Nicholls, J. N. *Adv. Inorg. Chem. Radiochem.* **1986**, *30*, 123.
(18) Bortoluzzi, M.; Ciabatti, I.; Femoni, C.; Funaioli, T.; Hayatifar, M.; Iapalucci, M. C.; Longoni, G.; Zacchini, S. *Dalton Trans.* **2014**, *43*, 9633.
(19) Ciabatti, I.; Femoni, C.; Iapalucci, M. C.; Ienco, A.; Longoni, G.; Manca, G.; Zacchini, S. *Inorg. Chem.* **2013**, *52*, 10559.
(20) (a) Schmidbaur, H.; Schier, A. *Chem. Soc. Rev.* **2012**, *41*, 370. (b) Chen, Z. N.; Zhao, N.; Fan, Y.; Ni, J. *Coord. Chem. Rev.* **2009**, *253*, 1. (c) Laguna, A. *Modern supramolecular gold chemistry: gold-metal interactions and applications;* Wiley-VCH: Weinheim, Germany, 2008. (d) Pyykkö, P. *Chem. Rev.* **1997**, *97*, 597.
(21) (a) Schmidbaur, H.; Schier, A. *Chem. Soc. Rev.* **2008**, *37*, 1932. (b) Katz, M. J.; Sakaib, K.; Leznoff, D. B. *Chem. Soc. Rev.* **2008**, *37*, 1884. (c) Schmidbaur, H. *Gold Bull.* **2000**, *33*, 3. (d) Kim, P. -S. G.; Hu, Y.; Brandys, M.-C.; Burchell, T. J.; Puddephatt, R. J.; Sham, T. K. *Inorg. Chem.* **2007**, *46*, 949.
(22) (a) Voβ, C.; Pattacini, R.; Braunstein, P. *C. R. Chim.* **2012**, *15*, 229. (b) Zank, J.; Schier, A.; Schmidbaur, H. *J. Chem. Soc., Dalton Trans.* **1998**, 323. (c) Fackler, J. P. *Inorg. Chem.* **2002**, *41*, 6959.
(23) (a) Schmidbaur, H. *Gold: Progress in Chemistry, Biochemistry and Technology;* Wiley: Chichester, U.K., 1999. (b) Scherbaum, F.; Grohmann, A.; Huber, B.; Krüger, C.; Schmidbaur, H. *Angew. Chem., Int. Ed.* **1988**, *27*, 1544. (c) Schmidbaur, H. *Chem. Soc. Rev.* **1995**, *24*, 391.
(24) (a) Muñiz, J.; Wang, C.; Pyykkö, P. *Chem.—Eur. J.* **2011**, *17*, 368. (b) Pyykkö, P. *Chem. Soc. Rev.* 2008, *37*, 1967. (c) Pyykkö, P. *Angew. Chem., Int. Ed.* **2004**, *43*, 4412. (d) Pyykkö, P.; Li, J.; Runeberg, N. *Chem. Phys. Lett.* **1994**, *218*, 133.
(25) Sculfort, S.; Braunstein, P. *Chem. Soc. Rev.* **2011**, *40*, 2741.
(26) Reina, R.; Riba, O.; Rossell, O.; Seco, M.; de Montauzon, D.; Pellinghelli, M. A.; Tiripicchio, A.; Font-Bardia, M.; Solans, X. *J. Chem. Soc., Dalton Trans.* **2000**, 4464.
(27) (a) Cordero, B.; Gómez, V.; Platero-Prats, A. E.; Revés, M.; Echevarría, J.; Cremades, E.; Barragán, F.; Alvarez, S. *Dalton Trans.* **2008**, 2832. (b) Bondi, A. *J. Phys. Chem.* **1964**, *68*, 441.
(28) Grimme, S. *J. Chem. Phys.* **2006**, *124*, 34108.
(29) Kowala, C.; Swan, J. M. *Aust. J. Chem.* **1966**, *19*, 547.
(30) Keller, E. *SCHAKAL99;* University of Freiburg: Germany, 1999.
(31) Sheldrick, G. M. *SADABS,* Program for empirical absorption correction; University of Göttingen: Germany, 1996.
(32) Sheldrick, G. M. *SHELX97,* Program for crystal structure determination; University of Göttingen, Germany, 1997.
(33) Frisch, M. J.; Trucks, G. W.; Schlegel, H. B.; Scuseria, G. E.; Robb, M. A.; Cheeseman, J. R.; Scalmani, G.; Barone, V.; Mennucci, B.; Petersson, G. A.; Nakatsuji, H.; Caricato, M.; Li, X.; Hratchian, H. P.; Izmaylov, A. F.; Bloino, J.; Zheng, G.; Sonnenberg, J. L.; Hada, M.; Ehara, M.; Toyota, K.; Fukuda, R.; Hasegawa, J.; Ishida, M.; Nakajima, T.; Honda, Y.; Kitao, O.; Nakai, H.; Vreven, T.; Montgomery, J. A., Jr.; Peralta, J. E.; Ogliaro, F.; Bearpark, M.; Heyd, J. J.; Brothers, E.; Kudin, K. N.; Staroverov, V. N.; Kobayashi, R.; Normand, J.; Raghavachari, K.; Rendell, A.; Burant, J. C.; Iyengar, S. S.; Tomasi, J.; Cossi, M.; Rega, N.; Millam, N. J.; Klene, M.; Knox, J. E.; Cross, J. B.; Bakken, V.; Adamo, C.; Jaramillo, J.; Gomperts, R.; Stratmann, R. E.; Yazyev, O.; Austin, A. J.; Cammi, R.; Pomelli, C.; Ochterski, J. W.; Martin, R. L.; Morokuma, K.; Zakrzewski, V. G.; Voth, G. A.; Salvador, P.; Dannenberg, J. J.; Dapprich, S.; Daniels, A. D.; Farkas, Ö.; Foresman, J. B.; Ortiz, J. V.; Cioslowski, J.; Fox, D. J. *Gaussian 09,* Revision D.01; Gaussian, Inc.: Wallingford, CT, 2009.
(34) Dolg, M.; Stoll, H.; Preuss, H.; Pitzer, R. M. *J. Phys. Chem.* **1993**, *97*, 5852.
(35) Gorelsky, S. I.; Lever, A. B. P. *J. Organomet. Chem.* **2001**, *635*, 187.